Program Digest, 2019 IEEE International Ultrasonics Symposium (IUS)
Glasgow, Scotland, October 6-9, 2019

Integrated High-performance Clocking Solutions Utilizing Mirror-encapsulated BAW Resonators

Ernest T.-T. Yen[1], Keegan Martin[2], Mahmud Chowdhury[3], Jeronimo Segovia-Fernandez[1], Danielle Griffith[4], Benyong Zhang[5], Nicholas Dellas[2], Trevor Tarsi[2], Django Trombley[2], Brian Goodlin[2], Ricky Jackson[2], Anindya Poddar[3], Baher Haroun[1], Ahmad Bahai[1]

[1]Kilby Labs / [2]ATD / [3]SCP / [4]EP-CMCU / [5]HSDC-CTS

Texas Instruments Inc.

Santa Clara, CA / Dallas, TX / Federal Way, WA

ernest.ttyen@ti.com

***Abstract*—This work introduces mirror-encapsulated BAW (bulk acoustic wave) resonators which include two sets of Bragg reflectors above and below the resonator body. This symmetrical DBAR (dual-Bragg acoustic resonator) stack offers extra design freedoms to alter resonator's acoustic properties. With this dual acoustic mirror structure, a DBAR requires no cavity on either side of the resonator and is still immune to mass loading effect from contamination and assembly. This advantage enables cost-effective system integration by directly marrying a DBAR and a CMOS die in a plastic package. System chips utilizing DBAR as the high-frequency clocking reference are demonstrated here. With compensation algorithm and careful design of the package, these DBAR-based clocking systems can achieve ±25 ppm stability over the entire operation temperature range, resulting industry's first crystal-less BLE chip.**

Keywords*—*BAW (bulk acoustic wave) resonator, DBAR (dual-Bragg acoustic resonator), MEMS, clocking, crystal-less, system-in-package integration

I. Introduction

Quartz crystals and oscillators (XOs) have dominated the timing reference market for almost a century since their invention in the 1920s [1]. These crystal oscillators have found utility in a wide range of products from low-end (real-time clock) to high-end (complex radio, GPS, and military/aero) applications due to their excellent frequency accuracy, low temperature drift, long-term stability, and low phase noise. However the bulky size and challenges to be integrated with CMOS process make crystals and XOs remain external components on board for most applications. The emerging 5G mobile communication and internet-of-things (IoT) markets have driven the search for new resonator technologies that consume lower power, with smaller form factor, for ease of integration, while maintaining similar or better performances a quartz crystal can offer. With the phase velocity in the order of a few thousands to tens of thousands meters per second, solid-state micro-resonator technologies provide promising solutions to realize these high-Q and high frequency references in compact sizes.

Micro-fabrication technologies facilitated the development of various µ-resonator technologies utilizing either capacitive [2-4] or piezoelectric [5-9] transductions. Capacitive resonators use electrostatic force to drive single- or poly-crystalline silicon resonators from kilohertz to tens of megahertz range with quality factor Q over 10,000 [2-4]. With frequency-quality factor product above 2×10^{13} Hz, pioneers have commercialized oscillators based on these resonators for timing applications and gained significant market share at low-end real-time clock market. However these products still serve as standalone oscillators on PCBs. On the other hand, piezoelectric resonators like SAW (surface acoustic wave) or BAW (bulk acoustic wave) technologies utilize AlN, ZnO, or $LiNbO_3$ thin film to achieve gigahertz operation frequencies and electromechanical couplings in the range of a few percent suitable for RF front-end filter applications. Among them, FBAR is fabricated by depositing the piezoelectric thin film and metal electrodes over a sacrificial layer, then selectively removing the sacrificial layer to leave a free-standing structure [7-8]; SMR and advanced SAW, on the other hand, use acoustic reflectors to prevent energy leakage into the substrate [9-10]. With f-Q product 5×10^{12} Hz, oscillators demonstrated with these high-frequency resonators also shows very low RMS jitter [11]. Reference [12] also announced standalone 32 kHz resonators as a direct quartz replacement for system-integration. However all these technologies require cavities on one or both sides of the resonator to provide proper acoustic isolation. These cavities affect robustness with respect to external forces and can cause non-linearity effect for certain high-power applications.

To date, system-in-package (SiP) integration using micro-acoustic resonators as reference clocking signals are still rare in the market. The primary reasons are believed to be: low mass production yield, limited compliance with customer-end package options, and small value add proposition of the products. Costs involving MEMS encapsulation are usually high and become a critical consideration for marketing products and devices with low fabrication cost. Moreover, neglecting system perspective during the early stages of technology development can result in unduly restrictive specifications and development delays. As a result, lessons learned throughout various technology developments all suggest to bring the system, circuit, and resonator designs and the package solution under one roof to advance high-margin and fully-integrated products.

Due to the challenges mentioned above, Texas Instruments started developing its own µ-resonator technology to be integrated with system chips. The following sessions will introduce this resonator technology, design, performance, and integration, followed by an oscillator topology that is suitable for low-power operations. System performance and advantages of using these integrated micro-acoustic resonators will be discussed at the end.

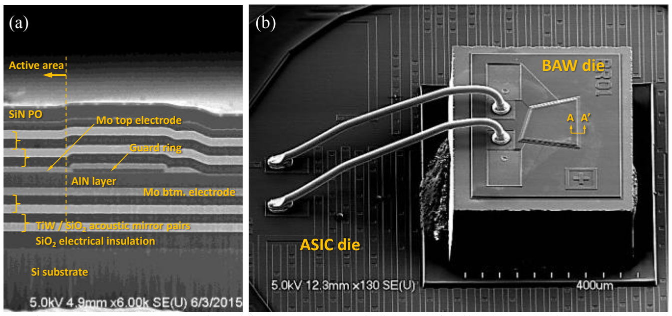

Fig. 1 (a) Cross-section along AA' and (b) stack die system-in-package integration of TI's dual-Bragg acoustic resonator.

II. Dual-Bragg Acoustic Resonator

Fig. 1 shows the cross-section and stack die integration of TI's mirror-encapsulated AlN BAW resonator. Similar to the SMR technology, TI's BAW resonator employs alternating high- and low-acoustic impedance layers beneath the device as the Bragg reflectors to prevent acoustic energy leakage into the substrate. Furthermore, acoustic mirrors are also placed on top of the resonator stack to protect the device and minimize energy leakage into the package materials. This multi-layer device confines acoustic energy in the Mo-AlN-Mo resonant body, allowing efficient excitation without the need of costly vacuum cavities around the resonator. As a result, this mirror encapsulated BAW resonator is immune to frequency drift caused by adsorption of surface contaminants and can be directly placed in a non-hermetic plastic package to enable system-in-package (SiP) integration with a minimum cost adder.

A. *Choice of Frequency*

TI's DBAR operates in the thickness mode and determines the operating frequency, to the first-order, by the Mo-AlN-Mo thin film thicknesses. For c-axis oriented Wurtzite crystalline AlN thin film, the longitudinal phase velocity is about 11,000 meters per second. With practical thickness in production, the frequency sweet spot of this technology is between 1 and 5 GHz. Consequently, oscillator architectures based on these high-frequency resonators typically require several stages of dividers to divide the output clock signal down to the frequency of interest. This is a fundamental difference from designing a quartz crystal-based oscillator, for which overtone and PLLs (phase-locked loops) are commonly used to multiply the clock signal to above tens of megahertz range.

B. *Tunability*

To achieve maximum effective electromechanical coupling coefficient K_{eff}^2, the Mo-AlN-Mo thickness ratio should be around 1:6:1 [13]. Owing to various limitations from early process integration, TI's 1st-generation BAW resonator does not follow this design principle. However with measured effective coupling K_{eff}^2 about 3.5 to 4.0% it is sufficient to calibrate fabrication frequency offset at final test.

C. *Co-optimized Acoustic Mirror Design*

The design of acoustic mirrors plays an important role to achieve high Q. Fig. 2 shows the calculated transmissivity of two pairs of TiW/SiO_2 acoustic mirrors optimized for quarter-wavelength longitudinal waves only (black) and co-optimized

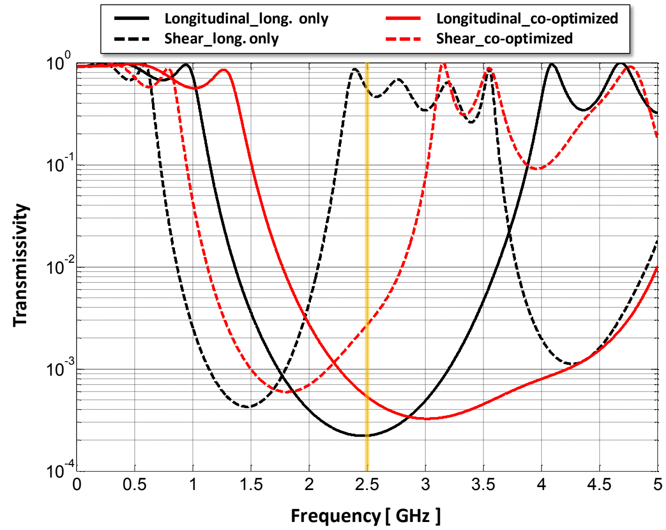

Fig. 2 Transmissivity of acoustic mirrors optimized for λ/4 longitudinal wave only (black) and co-optimized for both shear and longitudinal waves (red) at 2.5 GHz with 2 pairs of TiW/SiO_2 layers.

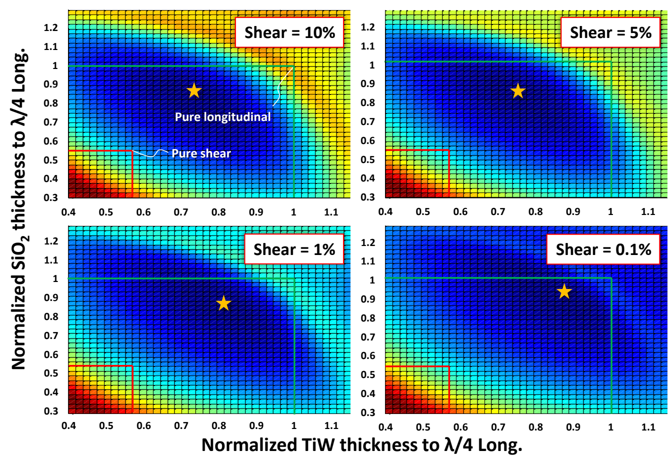

Fig. 3 Different shear wave contribution results in different TiW/SiO_2 thickness (normalized to quarter-wavelength) optimization. Star marks in each plot represent the minimum transmissivity for each case.

for both shear and longitudinal waves at 2.5 GHz [9]. It is worth noticing that this optimization is based on the assumption of known shear mode contributions. Resonators with different percentage of shear mode contribution require different TiW/SiO_2 thickness ratio. Fig. 3 shows the minimum transmissivity (dark blue) regions and its corresponding TiW/SiO_2 thickness for each case with different shear mode contribution.

D. *Spurious Mode Reduction*

DBAR is a type II resonator with the signature of spurious modes appear below the series resonance frequency f_s on a Smith circle [14]. In theory it requires a recessed guard ring (or frame) to increase the cut-off frequency at the edge of resonator thus reducing the impact of lateral spurious modes near resonance [15]. However, it was found that using a raised guard ring with optimized dimensions (thickness and width) and space between the edge of the resonator, one can still reduce spurious modes, achieve smoother Smith circle, and improve resonator's quality factor.

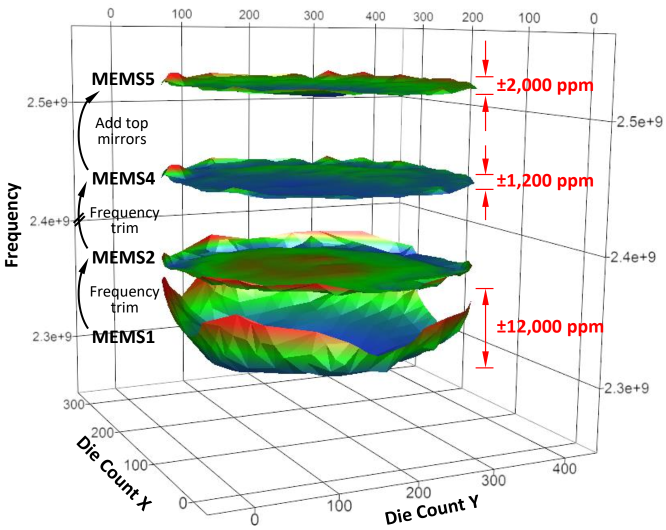

Fig. 4 The surface plots of cross-wafer frequency variation at different steps. The trimming technique removes materials locally to correct the frequency error.

E. *Frequency Trimming*

The operation frequency of a BAW resonator is determined by the film thickness used in the resonator stack. Transmission line theory and Mason model can effectively predict the 1D behavior [7-9]. The third column in Table I list the calculated frequency sensitivity of each layer over its thickness variations. In order to correct frequency errors caused by cross-wafer thickness variation, gradual in-line ion beam frequency trimmings are performed to locally remove different amount of materials after the initial probe. Fig. 4 shows surface plots of cross-wafer frequency data collected at different steps. Current baseline process is capable of tightening the frequency deviation from ±12,000 ppm at MEMS1 (initial probe) to less than ±1,200 ppm at MEMS4 (the last trim at top electrode), then increased to ±2,000 ppm at MEMS5 (after adding top mirrors without further trimming). Note that although more layers were added after MEMS4, MEMS5 is about 80 MHz *higher* than MEMS4. This is the clear evidence that top Bragg mirrors alter the acoustic characteristic of the entire resonator stack, rather than just serve as the protective overcoat to prevent contamination from package.

F. *Passive Temperature Compensation*

Frequency stability over temperature variation is another unavoidable challenge when developing a production-worthy resonator technology for timing applications. BAW resonators made of pure AlN thin film encounter more than 3,000 ppm frequency drift over the industrial temperature range due to AlN's 1st-order TCF of about −25 ppm/°C. Although this number is small compared to other materials, a passive temp compensation technique at material or device level is required.

Silicon dioxide thin film is well known for its mechanical stiffening behavior at elevated temperature (a positive TCF). By adding a correct amount of SiO_2 (TC-oxide) inside the BAW resonator, the overall 1st-order TCF of can be reduced to less than ±0.5 ppm/°C. The last column in Table I list the 1st-order TC sensitivity over thickness variation, indicating a 2.7 nm variation of TC-oxide thickness can cause the 1st-order TCF change by 1 ppm/°C. Note that TCF sensitivity over TC-oxide thickness variation is 2 to 3 orders higher than oxide layers used in acoustic mirrors. As a result, the TC-oxide thickness control is the most stringent step in the whole fabrication process and it requires extremely tight control over thin film thickness and thermo-mechanical properties accounting for within wafer, wafer-to-wafer, and lot-to-lot variations.

III. System Integration in Package

A. *Crystal-less SoC*

Fig. 5 shows the frequency reference system that enables crystal-less BLE-compliant wireless nodes. Typically, a BLE system requires two external quartz crystals: the high frequency one operating at 12 to 48 MHz to synthesize radio frequencies for various protocols; and the low frequency one running at 32 kHz to synchronize the data transmission between nodes. TI's new BLE chip omits both external crystals by integrating a DBAR-based clocking system to sustain ±25 ppm overall frequency stability [16]. The oscillator core is a complementary cross-coupled differential oscillator with a high-Q DBAR to replace commonly used parallel LC network. The oscillation occurs at DBAR's parallel resonance frequency at which the impedance magnitude is maximum to maintain sufficient voltage swing with low power consumption [17]. Another inherent advantage of this oscillator is the differential architecture which reduces radiated emissions and improves spur and coupling performance.

The digital PLL step size is 1.674 kHz, about 0.7 ppm for the 2.4 GHz RF band. A precise radio frequency F_{RF} for receiver (RX) and transmitter (TX) can be generated by adjusting the PLL's divide ratio to calibrate the initial offset and to actively compensate the drift of the reference clock F_{REF} over temperature variation, which results in ±25 ppm overall frequency stability to replace the 48 MHz external crystal [16]. On the other hand, the 32 kHz synchronization clock of accuracy better than ±500 ppm can be obtained by periodically calibrating the on-chip RC oscillator using the 48 MHz F_{RF} system clock mentioned above. The combination of these

TABLE I. FREQUENCY AND TEMPERATURE SENSITIVITY

LAYER NAME	MATERIAL	FREQ. SENSITIVITY MHz / nm	TEMP. SENSITIVITY nm / (ppm/°C)
Protective overcoat	SiN	0	--
Top oxide	SiO_2	-0.0006	-9,100
2nd top mirror pair	TiW	-0.0046	-1,201
2nd top mirror pair	SiO_2	-0.0203	-426
1st top mirror pair	TiW	-0.1188	-96
1st top mirror pair	SiO_2	-0.5085	-99
Top electrode	Mo	-2.1471	47
Temp. comp. oxide	SiO_2	-4.3506	2.7
Piezoelectric layer	AlN	-0.8618	378
Bottom electrode	Mo	-1.5662	-152
2nd bottom mirror pair	SiO_2	-0.3681	-82
2nd bottom mirror pair	TiW	-0.0856	-116
1st bottom mirror pair	SiO_2	-0.0142	-554
1st bottom mirror pair	TiW	-0.0028	-1,735
Base oxide	SiO_2	-0.0003	-23,529
Substrate	Si	0	--

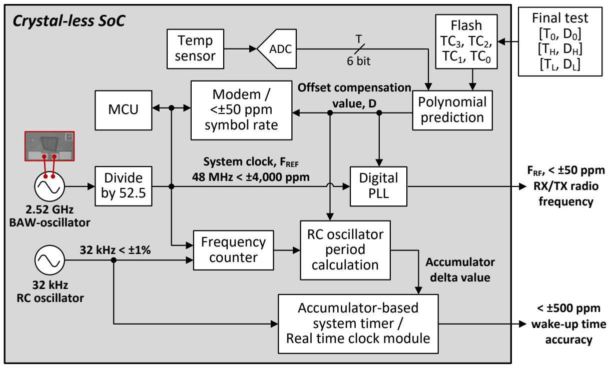

Fig. 5 Block diagram of the MEMS oscillator, divider, digital PLL, 32 kHz RC oscillator, and compensation method used to generate a crystal-less frequency reference system for a Bluetooth Low Energy radio.

techniques removes the need of external quartz crystals while still generating *both* clock signals needed for a BLE compliant radio. The stacked die integration of this DBAR and this BLE radio chip was shown in Fig. 1(a).

B. System Performance

Fig. 6(a) shows the measurement results of the 48 MHz reference clock frequency stability from 40 packaged parts. The initial offset of the reference frequency F_{REF} has been calibrated by D-PLL. A tri-temperature insertion at T_L, T_0, and T_H is also used to characterize their individual temperature response using a production tester. When active temperature compensation is disabled, the BAW-oscillator and divider generate an F_{REF} that varies 125 ppm from –40°C to 105°C. This is the temperature characteristic inherited from passively compensated BAW resonators. When active temperature compensation is enabled, the frequency stability is improved to better than ±10 ppm, leaving ample margin for aging and package stress induced frequency drift. Fig. 6(b) shows the frequency stability of this BLE radio chip under 1,500-g 0.5-ms mechanical shock test. The integrated DBAR version shows 3 times better shock resistance than its counterpart using an external crystal on the PCB.

IV. Conclusion

This paper introduced TI's BAW resonator technology utilizing two sets of Bragg reflectors below and above the resonator body. This symmetrical DBAR structure offers extra design freedoms to alter resonator's acoustic properties and prevents acoustic energy leakage into the substrate and the package mold compound. A DBAR's operation does not require a cavity around the resonator and is still immune to mass loading effect from contamination and assembly. This advantage enables cost-effect system-in-package integration. The design principles were discussed. A crystal-less BLE radio chip was demonstrated using an integrated DBAR clocking reference system. The reference clock stability of ±10 ppm over the entire operation temperature range was achieved by actively compensating the oscillator with a digital-PLL. It also showed better shock resistance than its counterpart using an external crystal on the PCB. This new micro-acoustic resonator technology has passed standard reliability tests and ready for mass production.

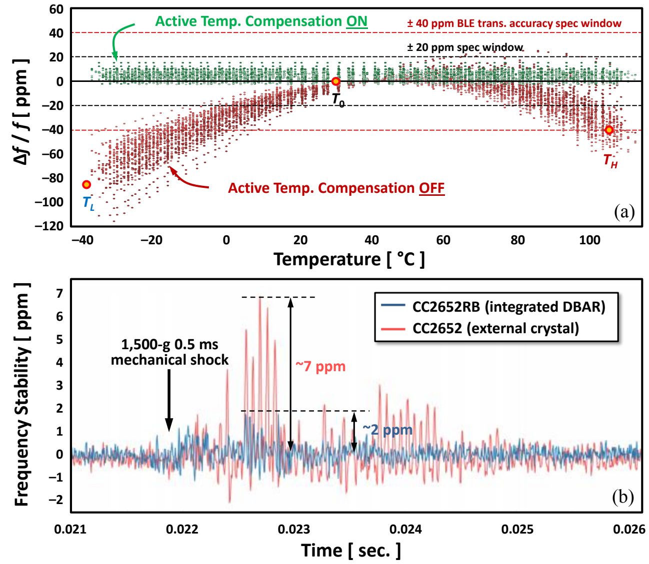

Fig. 6 (a) Temperature satbility of 48 MHz FRF generated from 2.52 GHz DBAR resonator. (b) Comparison of mechanical shock

Acknowledgment

The authors would like to thank engineers in the DHC and DFAB for their invaluable contributions to this work.

References

[1] G. W. Pierce, "Piezoelectric crystal resonators and crystal oscillators applied to the precision calibration of wavemeters", Proc. of the American Academy of Arts and Sciences, 59 (4): 81–106, 1923.

[2] C. T.-C. Nguyen and R. T. Howe, "An integrated CMOS micro-mechanical resonator high-Q oscillator", IEEE JSSC, Vol. 34, No. 4, 1999.

[3] SiTime website: www.sitime.com/technology/mems-oscillators

[4] W.-T. Hsu, "Vibrating RF MEMS for clock and frequency reference applications", Technical Digest, IMS, 2006.

[5] J. H. Kuypers, "High frequency oscillators for mobile devices", Piezoelectric MEMS Resonators, pp. 335-385, 2017.

[6] H. Bhugra et al., "Commercialization of world's first piezoMEMS resonators for high performance timing applications", Proc. IEEE MEMS, 2014.

[7] K. M. Lakin, G. R. Kline, and K. T. McCarron, "Development of miniature filters for wireless applications", IEEE Trans. Microwave Theory Tech. 43, 1995.

[8] R. Ruby, P. Bradley, D. Clark, D. Feld, T. Jamneala, and K. Wang, "Acoustic FBAR for filters, duplexers and front end modules", IEEE Microwave Symposium Digest, Vol. 2, 2004.

[9] S. Marksteiner, J. Kaitila, G. Fattinger, and R. Aigner, "Optimization of acoustic mirrors for solidly mounted BAW resonators", Proc. IEEE IUS, 2005.

[10] T. Takai et al., "Incredible high performance SAW resonator on novel multi-layerd substrate", Proc., IEEE IUS, pp 1-4, 2016.

[11] A. Nelson et al., "A 22 µW, 2.0 GHz FBAR oscillator", Proc. IEEE RFIC 2011.

[12] V. Kaajakari et al., "A 32.768 kHz MEMS resonator with ±20 ppm tolerance in 0.9 mm×0.6 mm chip scale package", Proc. IFCS 2019.

[13] K. M. Lakin et al., "Improved bulk wave resonator coupling coefficient for wide bandwidth filters", Proc. IEEE IUS, pp. 821-831, 2001.

[14] R. Ruby, "Review and comparison of bulk acoustic wave FBAR, SMR technology", Proc. IEEE IUS, PP. 1029-1040, 2007.

[15] J. Kaitila, M. Ylilammi, J. Ella, and R. Aigner, "Spurious resonance free bulk acoustic wave resonators", Proc., IEEE IUS, 2003.

[16] D. Griffith et al., "A crystal-less bluetooth low energy radio using a MEMS-based frequency reference system", Proc., EFTF/IFCS, pp. 181-184, 2017.

[17] R. Thirunarayanan et al., "Complementary BAW oscillator for ultra-low power consumption and low phase noise", Proc. NEWCAS 2011, pp. 97–100, 2011.